

# Effect of mix proportion on the uniaxial tensile properties of polypropylene fibre cementitious composites

Peiwen Wang<sup>1</sup>, Jiazuo Shao<sup>1</sup>, and Rui Guo<sup>1, 2</sup>

<sup>1</sup> School of Civil Engineering, Southwest Jiaotong University, Chengdu 610031, China;

<sup>2</sup> State Key Laboratory of Bridge Intelligent and Green Construction, Chengdu 611756, China.

**Abstract.** Numerous studies have proven that the incorporation of fibre-reinforced composites significantly increases the tensile strength of cement mortar. In this work, to further explore the influence laws of three factors, namely, the fly ash content, water-binder ratio, and sand-binder ratio, on the ultimate stress of polypropylene fibre cement-based composites (PP-FRCC) under uniaxial tension, a full-factorial design of experiments (DOE) was adopted to analyse the data. Each of the three selected factors had three levels and twelve repetitions. Analysis of variance (ANOVA) was used to determine the statistically significant effects among the overall means and whether there were interactions between the factors, establish the optimal mix proportion that best met the test requirements, and develop a prediction model for the tensile strength of PP fibre-reinforced, cement-based composites. The research results show that a change in the sand-binder ratio has a greater effect on the ultimate stress than does the fly ash content and that the fly ash content has a greater effect than does the water-binder ratio. However, all three factors have extremely significant effects on the ultimate stress. The interactions between the fly ash content and the water-binder ratio and between the fly ash content and the sand-binder ratio are extremely significant, whereas the interaction between the water-binder ratio and the sand-binder ratio is significantly influential. The sand-binder ratio is positively correlated with the ultimate stress of the composites, whereas the fly ash content and water-binder ratio are negatively correlated with the ultimate stress of the composites. The optimal tensile strength is obtained when the fly ash content is 0.35, the water-binder ratio is 0.27, and the sand-binder ratio is 0.84. The root mean square error (RMSE) of the radial basis function neural network (RBFNN) test set is 0.24197, and the coefficient of determination (R<sup>2</sup>) reaches 0.90, indicating that the model has strong explanatory power. This method is feasible, and its prediction accuracy meets engineering requirements, providing a new approach for investigating the strength of hybrid fibre-reinforced concrete in engineering.

**Keywords:** Polypropylene fibre cement-based composites (PP-FRCC), Full-factorial design of experiments (DOE), Tensile strength, Analysis of variance (ANOVA), Radial basis function neural network (RBFNN).

## 1. Introduction

Cementitious composites are extensively utilised in contemporary infrastructure construction, and their consumption is progressively increasing, with the performance requirements becoming increasingly stringent[1,2]. Nonetheless, owing to the inherent disadvantages of traditional cementitious materials, such as concrete and cement mortar, their relatively low tensile strength, poor acid resistance, poor heat resistance, and susceptibility to cracking when subjected to tensile stress caused by external forces, the further development of cementitious materials is greatly limited[3]. As numerous studies have shown, the incorporation of fibre-reinforced composites into cement mortar has been proven to increase the tensile strength, deformation resistance, and crack resistance of the mortar. This finding not only addresses the requirements of the specific project but also represents a highly effective approach to achieve the objective of producing high-performance cement composites. The research significance of this approach is significant and far-reaching[4,5].

Conventional fibre-reinforced cementitious composites (FRCC) typically employ polyvinyl alcohol (PVA) fibres as reinforcement composites, thereby significantly improving the performance of conventional cementitious materials through the reinforcing, toughening and crack-blocking effects of PVA fibres. However, the high cost of PVA fibres restricts the promotion and application of this material in civil engineering[6,7]. Polypropylene (PP) fibre is a low elastic modulus

synthetic fibre spun from isotactic PP. This fibre has many advantages, such as light weight, high strength, good flexibility, good electrical insulation, good corrosion resistance and very competitive low price[8].

Consequently, studies have attempted to use more cost-effective PP fibres as an alternative to PVA fibres in FRCCs[9]. Lin et al.[10] conducted mechanical property tests on hybrid PP-PVA-ECC and PVA-ECC. The results of the study revealed that an increase in the fibre volume ratio resulted in a decrease in compressive strength; however, the tensile and impact resistance of the PP-PVA-ECC was superior to that of the PVA-ECC. Saljoughian et al.[11] utilised substantial quantities of slag and PP fibres in fibre-reinforced concrete, thereby demonstrating that the tensile strains of ECC with elevated levels of slag and PP fibres attained or even exceeded those of conventional ECC comprising PVA fibres. By performing compression and flexural tests on concrete with different PP fibre admixtures, Wei Yimeng et al.[12] determined the effective upper limit of the PP fibre content. Mei Mengjun et al.[13] evaluated the mechanical properties of concrete with different fibre contents. The results show that steel fibres and PP fibres can significantly improve the tensile and flexural properties of concrete. Zhu et al.[14] proved that the incorporation of 2% PP fibres and 60% fly ash into the cement matrix resulted in better crack resistance and flexural toughness than ordinary concrete did by analysing the compressive and flexural properties of PP fibre-reinforced, cement-based composites. In summary, the current research on the mechanical properties of PP fibre-reinforced, cement-based composites is mostly in the form of PP fibres compounded with other fibres, and the existing research has focused mainly on improving their compressive and flexural properties. Relatively few studies address the tensile properties of these composites. Therefore, examining the tensile properties of cement-based composites constructed of single-doped PP fibres is highly important.

In summary, under the condition of only adding PP fibres, this paper uses three-factor and three-level full-factorial design of experiments (DOE) to design 27 groups of polypropylene fibre cement-based composites (PP-FRCC) with different ratios for uniaxial tensile tests. The effects of three variables, i.e., the fly ash content, water-binder ratio and sand-binder ratio, on the tensile properties of PP-FRCC were investigated, and the optimal mixing ratio was established to meet the test requirements. On this basis, a radial basis function neural network (RBFNN) was established to predict the strength of PP-FRCC.

## 2. Experimental program

### 2.1 Full-factorial test scheme

#### 2.1.1 DOE

DOE is predicated on the comprehensive evaluation of the effect of each factor on the test results by combining all levels of each factor in the test.

The main focus of this paper is the effect of the mixing proportion on the tensile properties of PP-FRCC. For cementitious materials, three proportions, namely, the ratio of fly ash to cement, the water-binder ratio and the ratio of sand-binder to cementitious materials, have a greater effect on the tensile properties of fibre-reinforced cement composites. A review of the literature revealed that researchers and scholars from various countries have formulated fibre cementitious composites with completely different dosages of quartz sand and fly ash; some scholars have doped with a very low dosage of quartz sand, at only 36%[15], but have also doped with a high dosage of quartz sand, at 100%[16]; some scholars have doped with a very low dosage of fly ash[17], at only 20% in China, but they have doped with a high dosage of fly ash, at 60%-80%[18]. Combining earlier research and related references, three variables (fly ash dosage, water-binder ratio, and sand-binder ratio) were defined as 3 factors, each of which had 3 levels of numerical variation, and the factor levels are shown in Table 1. Through the principle of DOE, considering various factors, 27 groups of different

mix ratio tests are designed, as shown in Fig 1. In this work, the fibre volume content is 2% of the total mass, and the water reducing agent constitutes 0.3% of the mass of the cementitious materials.

Table 1. Test factor level

Level	Factor		
	Fly ash dosage (%)	Water-binder ratio (%)	Sand-binder ratio (%)
1	0.35	0.27	0.36
2	0.50	0.30	0.60
3	0.80	0.33	0.84

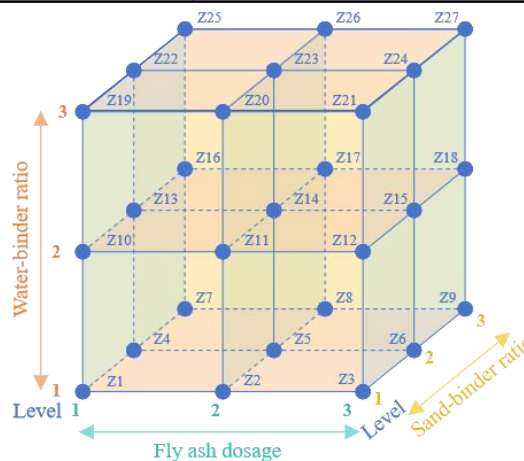


Fig. 1 Mix proportions of DOE

2.1.2 Analysis of the DOE

The present paper details the design of a three-factor, three-level DOE, incorporating 27 sets of mixing proportions. The fly ash admixture, water-binder ratio, and sand-binder ratio were designated Factors A, B, and C, respectively. The role of test factor effects is shown in Table 2.

Table 2. Function of the test factor effects

Main effect	A	B	C
Two-way interaction	AB, AC	BC	-
Triple interaction	ABC	-	-

2.2 Properties of the materials

The cement employed in this study was grade 42.5 ordinary Portland cement produced by the Sichuan Easheng Cement Group Company, with a density of 3.1 g/m<sup>3</sup> and a specific surface area of 3600 m<sup>2</sup>/g. The fine aggregate was 100 mesh quartz sand. The fly ash was first-grade fly ash. The mixed water used in this study was tap water from Qingbaijiang District, Chengdu city, Sichuan Province. A polycarboxylate superplasticiser was selected as the water reducing agent. PP was produced by a company in Hebei Province, and its monofilament diameter was 26 μm. The basic mechanical properties of the fibres are shown in Table 3.

Table 3. Physical and mechanical properties of the PP fibres

Type of fibre	Density (g/cm <sup>3</sup> )	Length (mm)	Elastic modulus (GPa)	Tensile strength (MPa)	Ultimate elongation in percent (%)
PP	0.91	12	5.7	570	25

### 2.3 Experimental design and methods

#### 2.3.1 Production and maintenance of the samples

Combined with existing experimental research on the tensile properties of PP-reinforced cement-based composites and the actual situation of our laboratory, a dumbbell-shaped (80 mm×30 mm×13 mm) mould was designed. The dimensional design of the sample for the PP-FRCC fit test is shown in Fig. 2. The sample production process is shown in Fig. 3. The process of sample fabrication involves pouring, covering the membrane, demoulding, and maintaining the bucket for 28 d.

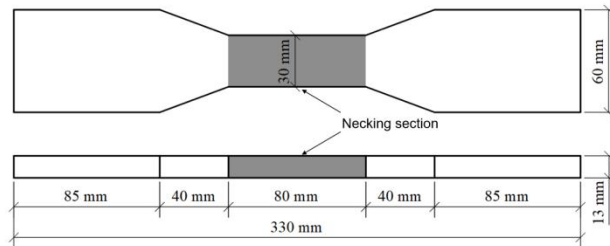


Fig. 2 Sample size

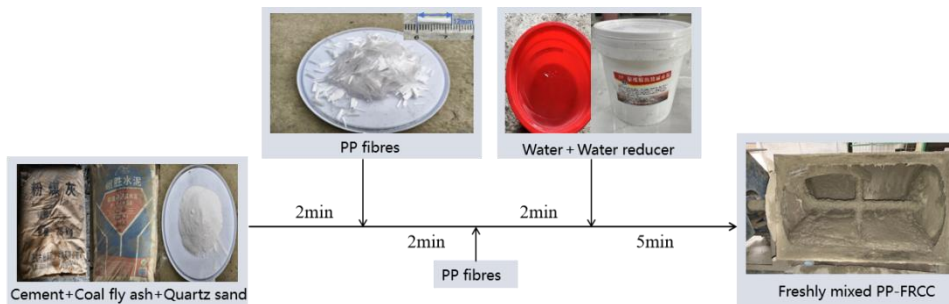


Fig. 3 Sample mixing process

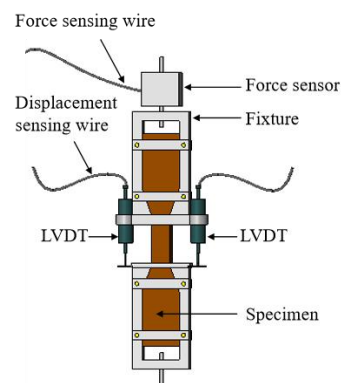
#### 2.3.2 Uniaxial tensile test

The loading method of the ‘dumbbell’ sample meets the relevant provisions of the Chinese code “Concrete Structure Test Method Standard” (GB/T 50152-2012)[19] and “High Ductile Fibre-Reinforced Cementitious Composites Mechanical Properties Test Method” (JC/T 2461-2018)[20]. The test data were collected by a TST3822E static strain testing and analysing system, the load and displacement were read by a force transducer and displacement transducer, respectively.

The test loading equipment used for the 'dumbbell' sample was a tensile testing machine. The maximum range of the testing machine is 5000 kN, which meets the tensile test conditions of PP-FRCC. For the experiment, the displacement loading control mode was used at a speed of 0.3 mm/min. The displacement sensors were arranged on both sides of the component to measure and record the displacement of the tensile interval, and the strain of the tensile zone was calculated. The test device is shown in Fig. 4.



(a) Testing machine



(b) Schematic diagram of specimen loading

Fig. 4 Loading equipment

### 3. Experimental results and analysis

#### 3.1 Experimental results

##### 3.1.1 Test process and phenomenon

Uniaxial tensile tests were conducted on 27 groups of 'dumbbell-shaped' samples with different mix proportions. Each group contained 12 dumbbell-shaped samples. The formation of multiple cracks was not observed. After the initial cracks formed, the main cracks developed around them, and the samples were eventually damaged by the continuous expansion of the main cracks. The samples exhibited ductility at the time of destruction; however, they did not exhibit the strain hardening phenomenon. The maximum tensile strength of the Group 7 samples was 5.219 MPa, whereas the standard value of axial tensile strength for ordinary C30 concrete material was 2.01 MPa. Consequently, the ultimate strength of the PP-FRCC prepared in this test was two to three times greater than that of ordinary concrete. The findings indicate that the fitment ratio of the Group 7 samples is excellent, and high-strength PP-FRCC were prepared.

##### 3.1.2 Tensile stress-strain curves

Typical PP-FRCC axial tensile stress-deformation curves for different fitment ratios in 27 sets of DOE are given in Fig. 5. When combined with the analyses of tensile stress-strain curves and section damage, the whole process of PP-FRCC axial tensile testing can be divided into two stages, as shown in Fig. 6.

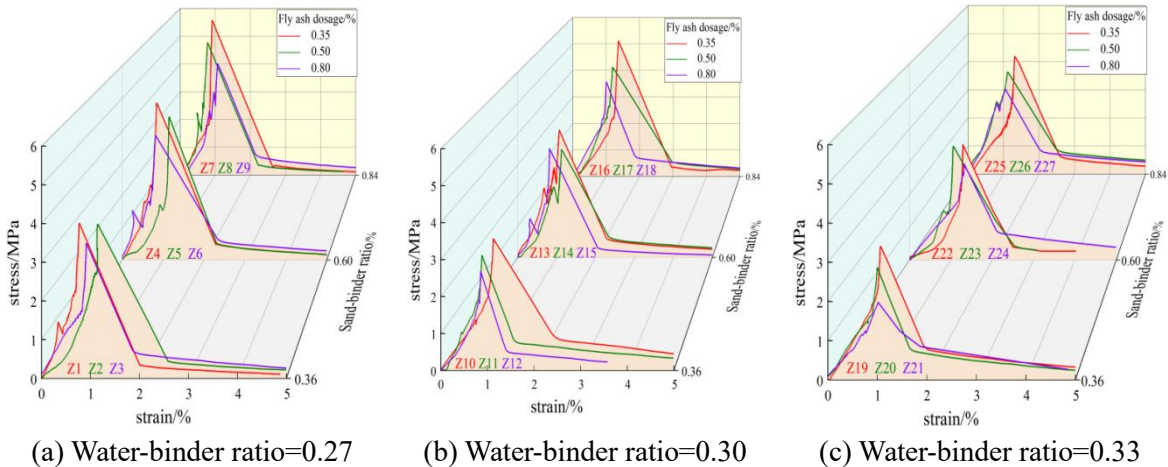


Fig. 5 Uniaxial tensile stress-strain curve of PP-FRCC

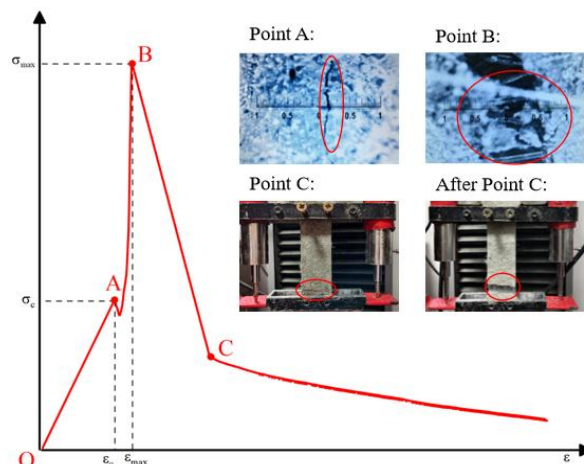


Fig. 6 Whole axial tensile process of PP-FRCC

Note:  $\sigma$  represents the stress,  $\varepsilon$  denotes the strain,  $\sigma_c$  indicates the initial cracking strain,  $\varepsilon_c$  represents the initial cracking strain,  $\sigma_{max}$  denotes the peak stress, and  $\varepsilon_{max}$  indicates the peak strain.

The OB segment is the linear elasticity stage, and this stage is divided into two small stages. The first stage is the OA stage, in which the stress increases slowly, the force is small, and the stress and strain satisfy a linear relationship, mainly because the cementitious matrix can withstand the tensile force. Owing to the occurrence of elastic deformation within the matrix, the PP fibres within the matrix are in a slight tensile state, and no cracks appear on the surface of the sample. Thus, the toughening and crack-resisting effects of PP fibres are not fully exerted at this stage. The sample exhibits an initial microcrack at point A, but the crack does not penetrate, and the fibres begin to bear external forces. The second stage is the AB section. At this stage, the stress and strain still have a linear relationship. The stress increases rapidly, and the fibres and the matrix collaborate. At this stage, the microcracks of the concrete begin to merge to form macrocracks, but the stress in the matrix is transferred to the fibres in the cracks of the sample. The fibres are connected to the matrix on both sides of the crack by tension, and the uncracked matrix on both sides can continue to bear a certain load. When the peak stress (point B) is reached, a stable crack is formed, and the crack penetrates the whole matrix.

The BC section is a softening failure stage. After peak point B, the stress decreases rapidly, and the strain continues to increase. With the expansion of the main cracks on the surface of the sample, the proportion of the cement matrix that bears the load continues to decrease, and the proportion of the fibres that bear the load continues to increase. This stage pp plays a major role. After yield point C, the stress-strain curve of PP-FRCC gradually decreases and tends to be gentler. At this stage, when the matrix is completely broken, most of the fibres are still not broken, and the PP fibres bear all the load. If the load continues, the matrix crack further expands because of the large elastic modulus of the fibre itself. An increasing number of fibres are pulled out or broken with the 'hissing' tearing sound, ensuring the stability of the crack propagation at the fracture site, indicating that the fibres themselves have good ductility.

The above phenomenon can be explained by the finding that the PP fibres are uniformly dispersed. Because its tensile strength is much greater than the tensile strength of the matrix, the PP fibre can effectively inhibit the expansion of tensile cracks in the PP-FRCC so that the matrix of the PP-FRCC can still have a certain binding effect when the surface layer cracks under the bonding effect of the PP fibres.

### 3.2 Effects of different mixing ratios on strength

Uniaxial tensile tests were conducted on 27 groups of PP-FRCC samples with different mix ratios. Each group of samples contained 12 dumbbell-shaped samples, and the 12 obtained ultimate tensile strength values of each group were analysed.

#### 3.2.1 Range analysis

In polar analysis, also known as intuitive analysis, the test results are simply analysed by calculating the polar deviation of the test data. First, the sum of the test data  $X_i$  was calculated for each group of replicate tests. Second,  $K_i$ ,  $k_i$  and the extreme difference  $R$  were calculated according to the data processing method of polar analysis; the calculation results are shown in Table 4.

Table 4. Limit stress range analysis data calculation

Number	Fly ash dosage (%)	Water-binder ratio (%)	Sand-binder ratio (%)
$K_1$	470.15	452.00	357.75
$K_2$	414.93	426.22	417.26
$K_3$	365.30	372.16	475.37
$k_1$	4.35	4.19	3.31
$k_2$	3.84	3.95	3.86

$k_3$	3.38	3.45	4.40
$R$	0.97	0.74	1.09

Note:  $K_i$  denotes the sum of the test results corresponding to each factor when the factor is taken at level  $i$ , that is,  $K_i = \sum x_{ij}$ , where  $x_{ij}$  denotes the test result corresponding to the level taken at Row  $i$  on the factor in Column  $j$  of the DOE table.  $k_i$  denotes the arithmetic mean of  $K_i$  at the same factor level;  $R$  denotes the extreme deviation.

The  $R$  value is the extreme difference of each factor, and the size of the  $R$  value can be used to determine the effect of the factor on the test results; a larger extreme difference indicates that the factor is more important. Therefore, Table 6 shows that the effect of the sand-binder ratio on the ultimate stress is greater than that of the fly ash dosage and that of the fly ash dosage is greater than that of the water-binder ratio.  $k_i$  is the average of the level of each factor; for the PP-FRCC "dumbbell" type samples, the greater the ultimate stress is, the better. Therefore, according to the  $k$  value of each factor, it can be concluded that the fly ash doping is at level 1, the water-binder ratio is at level 1, and the sand-binder ratio is at level 3. At this time, the full-factor stress limit analysis of the PP-FRCC can be performed to determine the optimal level from the extreme difference.

### 3.2.2 ANOVA

The ANOVA results of the ultimate stress are shown in Table 5. Table 5 shows that the main factors of the fly ash content, sand-binder ratio and water-binder ratio have a particularly significant effect on the ultimate stress of the PP-FRCC. The interaction effect of the water-binder ratio\*fly ash content and the sand-binder ratio\*fly ash content is particularly significant. The interaction effect of the fly ash content\*water-binder ratio\*sand-binder ratio is also particularly significant. The interaction effect of the sand-binder ratio\*water-binder ratio is significant. Moreover, through the mean square, the variation in the level of each factor affects the ultimate stress of the composites in the order of the sand-binder ratio>fly ash admixture>water-binder ratio, which is consistent with the conclusions obtained from the range analysis.

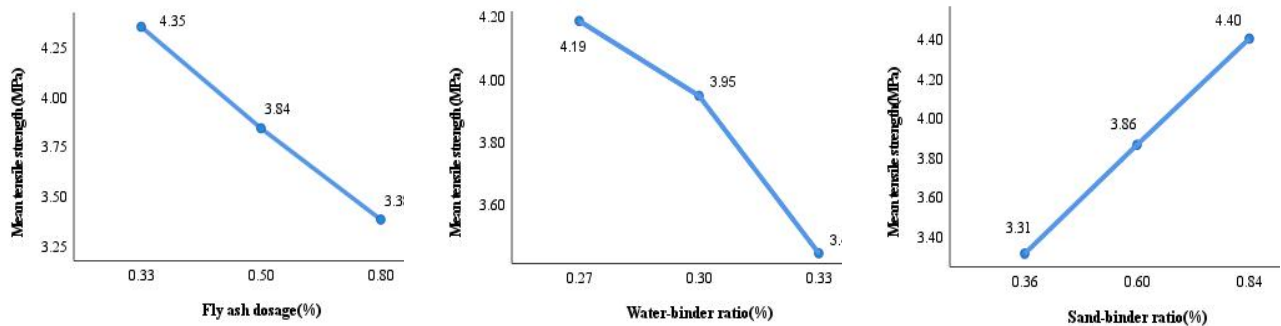
Table 5. Limiting stress ANOVA table

Variable	SS	DF	MS	F value	P value	Significance
Fly ash dosage	50.992	2	25.496	333.824	<0.001	**
Water-binder ratio	30.802	2	15.401	201.649	<0.001	**
Sand-binder ratio	64.106	2	32.053	419.678	<0.001	**
Water-binder ratio*Fly ash dosage	1.593	4	0.398	5.215	<0.001	**
Sand-binder ratio*Fly ash dosage	3.262	4	0.815	10.677	<0.001	**
Sand-binder ratio*Water-binder ratio	0.975	4	0.244	3.192	0.014	*
Fly ash dosage* Water-binder ratio * Sand-binder ratio	1.821	8	0.228	2.980	0.003	**
Error	22.683	297	0.076	-	-	-
Total	5001.775	324	-	-	-	-

Note: The four cases for defining the effect of the factors are as follows:(1) When  $F > F_{0.001}$ , the effect of the factors is particularly significant and is recorded as "\*\*".(2) When  $F_{0.01} \geq F > F_{0.05}$ , the effect of the factors is significant and is recorded as "\*".(3) When  $F_{0.05} \geq F > F_{0.01}$ , the representation factor has a certain effect and is recorded as ".".(4) When  $F_{0.1} \geq F$ , there is no effect of the factors on the test results.

#### (1) Main effects

The main effect is the effect of each individual factor at each level on the dependent variable without considering the other factors. A plot of each individual factor against tensile strength was created, as shown in Fig. 7.



(a) Main effects plot for fly ash dosage

(b) Main effects plot for water-binder ratio

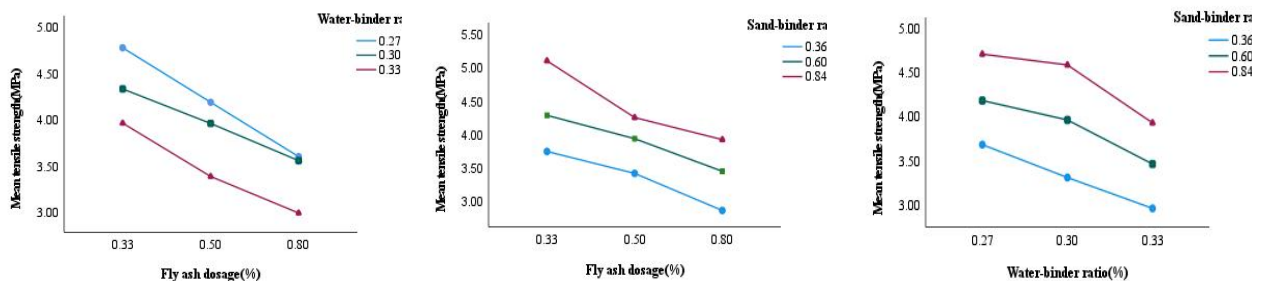
(c) Main effects plot for sand-binder ratio

Fig. 7 Main effects plot

The main effect curve shows the effect of the factor level on the ultimate stress of the PP-FRCC. As shown in Fig. 7(a), an increase in the fly ash content reduces the ultimate stress of the PP-FRCC. The selection of a fly ash content of 0.33 can increase the tensile strength of the PP-FRCC. The decrease in fly ash content is due to the increase in cement in cementitious materials. Cement plays a cementing role in the cement matrix, and cement directly affects the strength of materials. Therefore, an increase in the amount of cement will increase the ultimate stress of materials. As shown in Fig. 7(b), with increasing water-binder ratio, the tensile strength decreases. When the water-binder ratio increases from 0.30 to 0.33, the tensile strength changes drastically, and the change in tensile strength from this interval is 0.5 MPa. From 0.27 to 0.30, the increase in tensile strength is greatly reduced. In this interval, the increase in tensile strength is only 0.24 MPa. In the range from 0.27 to 0.30, the decrease in tensile strength is reduced by 50% compared with that in the range from 0.30 to 0.33. Therefore, the effect of the water-binder ratio on the ultimate stress of the material is not obvious within a certain range. The maximum significant difference occurs in the range of 0.30 to 0.33, and 0.27 is the best water-binder ratio for PP-FRCC. As shown in Fig. 7(c), with increasing sand-binder ratio, the ultimate stress of the material gradually increases, which is closely related to the skeleton role of the quartz sand in the cement matrix. There are no coarse aggregates in the PP cement matrix, so the effect of fine aggregate quartz sand on the strength is more obvious.

(2) Interaction plots (two-way interactions)

Two-way interactions are those in which one factor in combination with another factor produces a different effect than the effect of one factor only on material properties. For example, the water-binder ratio\*fly ash dosage pair produces different results than the effects of the fly ash dosage or the water-binder ratio only on the tensile strength. The interaction is plotted in Fig. 8.



(a) Water-binder ratio\*Fly ash dosage

(b) Sand-binder ratio\*Fly ash dosage

(c) Sand-binder ratio\*Water-binder ratio

Fig. 8 Interaction plots

Fig. 8 shows that there is an interaction between the parameters when the lines are not parallel. Fig. 8(a) shows that there is an interaction between two factors, the fly ash dosage and the

water-binder ratio, as the blue line is not parallel to the red and green lines. This finding is consistent with the conclusion that the p value of the interaction between the fly ash dosage and the water-binder ratio is less than the 0.05 level of significance in Table 7. Fig. 8(a) shows that at fly ash dosage of 0.8,  $p=0.506>0.05$ , for the two factors of a water-binder ratio of 0.27 and a water-binder ratio of 0.30, there was no significant difference. The preparation of PP-FRCC of this strength at a fly ash dosage of 0.8 can be considered in the direction of material savings by using a water-binder ratio of 0.27 rather than 0.30, and all other combinations of level parameters significantly differ. For this parameter combination, the strongest tensile strength of 4.77 MPa is produced for a fly ash dosage of 0.33 and a water-binder ratio of 0.27. This is because the strongest tensile strength also occurs at a fly ash dosage of 0.33 and a water-binder ratio of 0.27 under the main effect.

Fig. 8(b) shows that there is an interaction between two factors, the addition of fly ash and the sand-binder ratio, as the blue line is not parallel to the red and green lines. The reported p value of less than 0.05 confirms that there is indeed an interaction. The figure clearly shows that the reduction in tensile strength is significantly greater when the fly ash content is between 0.33 and 0.50 and the sand-binder ratio is 0.84 than at the other levels of sand-binder ratio, indicating that the interaction between the fly ash content and the sand-binder ratio is significantly greater at a sand-binder ratio of 0.84 than at 0.33 and 0.50. Notably, the tensile strength increases with increasing sand-binder ratio under the main effect of fly ash dosage. The highest combination of these parameters occurred with the combination of a sand-binder ratio of 0.84 and a fly ash dosage of 0.33.

Fig. 8(c) shows that the optimum combination was a water-binder ratio of 0.27 and a sand-binder ratio of 0.84. Producing the PP-FRCC at a higher sand-binder ratio results in a greater tensile strength, and when combined with the results for the water-binder ratio, the optimum water-binder ratio is 0.27 because the tensile strength tends to decrease as the water-binder ratio increases. In Fig. 8(c), when the sand-binder ratio is 0.84, there is no significant difference between the two factors, i.e., a water-binder ratio of 0.27 and a water-binder ratio of 0.30 ( $P=0.061>0.05$ ), whereas there are significant differences in the other parameter combinations.

Combined with range analysis and ANOVA, in the comprehensive analysis, when the fly ash content and water-binder ratio are at level 1 and the sand-binder ratio is at level 3, the tensile strength of the PP-FRCC full-factorial mix ratio test reaches the maximum.

#### 4. Neural network prediction

Strength is one of the most important properties of concrete. Recently, scholars worldwide have increasingly used neural networks for engineering prediction and structural damage identification; in particular, the BP network, as the core of the feed-forward network, has been widely used in concrete strength prediction[21]. Despite the widespread utilisation of the BP algorithm and its robust structural foundation, it is imperative to acknowledge its inherent limitations. Primarily, the training process of the algorithm engenders uncertainty owing to its comparatively gradual convergence and the inability to provide theoretical guidance for the selection of network parameters, such as the number of nodes in the hidden layer. This deficiency can result in convergence of the algorithm to local minima, thereby amplifying the error. The radial basis function neural network (RBFNN) has the capacity to determine the corresponding network topology according to the specific problem. The RBFNN is characterised by its ability to self-learn, self-organise and self-adapt, and it consistently approximates nonlinear continuous functions. The network is capable of rapid learning and training, and it can perform a wide range of data fusion and process data at a high speed. The superior properties of the RBFNN have resulted in its increased utilisation in a variety of fields, superseding the conventional back-propagation (BP) neural network. In this paper, the focus is on the utilisation of the RBFNN for the prediction of concrete strength[22-24].

### 4.1 Principle of the RBFNN

The RBFNN is a type of local approximation feedforward network that introduces a radial basis function into a neural network. The output of the RBF network is linearly related to the weights. A linear algorithm that guarantees global optimisation can be employed; concurrently, the training process is rapid, independent of the initial weights, and there is no local optimum problem. When the centre of the radial basis function of the network is appropriately chosen, a good approximation can be obtained with a very small number of neurons. The network structure is shown in Fig. 9.

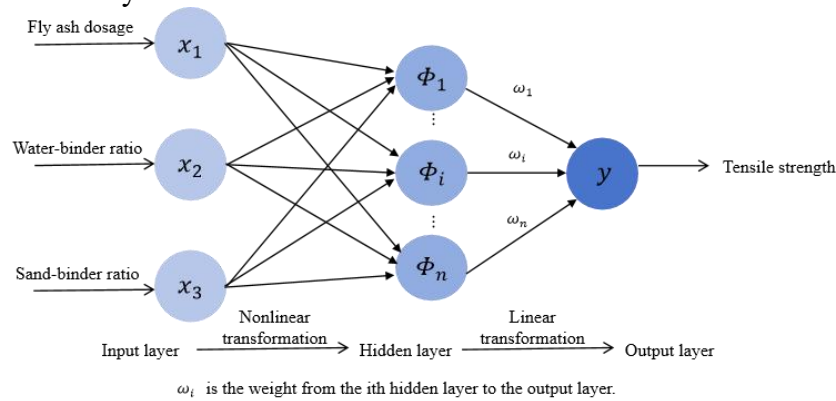


Fig. 9 RBFNN structure

### 4.2 Test of prediction results

With the RBFNN model established above, the simulated prediction results for the training and test sets were derived separately, and the relative errors between the predicted values and the true values of the trials were calculated and are summarised in Table 6. The root mean square error (RMSE) comparison between the true values and the predicted values of the training and test sets during network training is shown in Fig. 10.

Table 6. Analysis of the RBFNN model prediction results

Dataset	R2	MAE	MBE
Training set	0.86099	0.20902	1.6958e-3
Testing set	0.90068	0.19425	0.015412

The data in Table 6 and Fig. 10 indicate that the predicted value of the PP-FRCC strength RBFNN prediction model on the training set and the test set is highly consistent with the real value. Only a few extreme data deviate from the real value, indicating that the data dispersion is small, the fluctuation is not obvious, and it is closer to the real value, which further indicates that the predicted value of the RBFNN model has a small deviation from the measured value and that the model training effect is good. The RMSE of the test set is 0.24374, and the R2 reaches 0.90, indicating that the model has strong explanatory power and can be effectively applied to predict the strength of PP-FRCC.

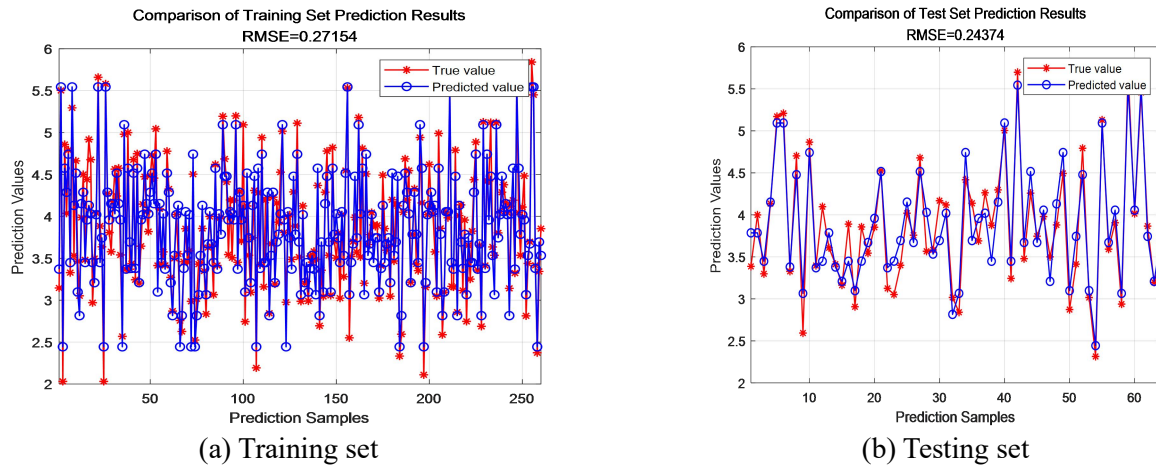


Fig. 10 Comparison between the predicted value of the RBFNN and the real value

## 5. Conclusion

(1) In this work, the DOE method is used to perform uniaxial tensile tests on 27 groups of PP-FRCC with different mix ratios, and 6 stress-strain curves and 12 tensile strength values are obtained for each group. The range analysis reveals that the effect of the change in the sand-binder ratio on the ultimate stress is greater than that of the fly ash content, which is greater than that of the water-binder ratio. In terms of ANOVA, the influence law of the three factors is consistent with the range analysis. The F value of the sand-binder ratio is greater than the F value of the fly ash content is greater than the water-binder ratio, but the effect of the three factors on the ultimate stress is particularly significant. The interaction effects of the water-binder ratio\*fly ash content and the sand-binder ratio\*fly ash content are particularly significant, and the interaction effects of the sand-binder ratio\*water-binder ratio are significant.

(2) According to the ANOVA results, the ultimate stress of the PP-FRCC gradually increases with increasing sand-binder ratio. A decrease in the fly ash content significantly increases the ultimate stress of the PP-FRCC. With increasing water-binder ratio, the tensile strength decreases, and the change in the water-binder ratio within a certain range has no obvious effect on the ultimate stress of the PP-FRCC. Combined with range and variance analyses, the optimal mix ratio was obtained for each group of tests. When the fly ash content and water-binder ratio were set at level 1 and the sand-binder ratio was set at level 3, the maximum tensile strength of the PP-FRCC composites was reached.

(3) Combined with the analysis of the tensile stress-strain curve and section failure of PP-FRCC, it can be seen that PP-FRCC experiences brittle fracture, and the maximum ultimate tensile strength is approximately 5.2 MPa. The tensile test process of the PP-FRCC sample can be divided into two stages: linear elasticity and softening failure.

(4) The RBFNN model established in this study can accurately and quickly predict the tensile strength of PP-FRCC, and the overall prediction effect is more accurate. The study shows that the RBFNN can be effectively used for predicting the strength of fibre-reinforced concrete and can be continuously learned by increasing the number of samples of experimental data to improve the network accuracy and generalisability and to establish a more perfect prediction system with greater value for engineering applications.

## Acknowledgment

This work was supported by the National Natural Science Foundation of China (Grant Number: 52378317).

## References

- [1] Hasan, Kamrul, Jaya, Ramadhansyah Putra, Yahaya, Fadzil Mat. Application of bentonite in cement-based composites: A review of current status, challenges and future prospects[J].JOURNAL OF BUILDING ENGINEERING,2024,98.
- [2] Amran, Mugahed,Huang, Shan-Shan,Onaizi, Ali M., et al. Recent trends in ultra-high performance concrete (UHPC): Current status, challenges, and future prospects[J].ONSTRUCTION AND BUILDING MATERIALS,2022,352,(0).
- [3] Sukanta Kumar Mondal. Sustainable cementitious materials for building and sorption applications[D].Missouri University of Science and Technology,2024.
- [4] Yao, Shun,Hu, Chuanlin,Wang, Fazhou, et al. Improving the interfacial properties of PVA fiber and cementitious composite: Design and characterization[J].CONSTRUCTION AND BUILDING MATERIALS,2023,409.
- [5] Qing, Longbang,Sun, Honglei,Zhang, Yuebo, et al. Research progress on aligned fiber reinforced cement-based composites[J].CONSTRUCTION AND BUILDING MATERIALS,2023,363.
- [6] Zhang, Ziyi, Ji, Yongcheng, Ji, Wenhao. Durability Performance Investigation for Engineering Fiber Cementitious Composites (ECC): Review[J].POLYMERS,2023,15,(4):931-931.
- [7] Liao, Weibin,Wu, Peizong,Huang, Jiatao, et al. Cost-Effective Engineered Cementitious Composites with Hybrid PVA and Basalt/PP Fiber: A Study on Compressive, Tensile and Impact Performance[J].MATERIALS,2023,16,(14):5172.
- [8] Wu, Heyang,Lin, Xiaoshan, Zhou, Annan. A review of mechanical properties of fibre reinforced concrete at elevated temperatures[J].CEMENT AND CONCRETE RESEARCH,2020,135,106117-106117.
- [9] Hu, Shi,Cai, Haibing,Hong, Rongbao, et al. Performance Test and Microstructure of Modified PVC Aggregate-Hybrid Fiber Reinforced Engineering Cementitious Composite (ECC)[J].MATERIALS,2021,14,(8):1856.
- [10] Saljoughian, Alireza, Bahmani, Hadi, Ansari, Zeynab, et al. An eco-friendly ECC with high slag and polypropylene fiber content for high-tensile strain applications[J].JOURNAL OF BUILDING ENGINEERING,2024,91.
- [11] Wei Yimeng et al. Experimental Study on Compressive and Flexural Performances of Polypropylene Fiber-Reinforced Concrete[J].Geofluids,2022,2022(1).
- [12] Mei Mengjun et al. Mechanical properties of nano SiO<sub>2</sub> and fiber-reinforced concrete with steel fiber and high performance polypropylene fiber[J].Materials Research Express,2021,8(10).
- [13] Zhu, Deqi,Tang, Aiping,Wan, Congli, et al. Investigation on the flexural toughness evaluation method and surface cracks fractal characteristics of polypropylene fiber reinforced cement-based composites[J].JOURNAL OF BUILDING ENGINEERING,2021,43.
- [14] Lin, Jia-Xiang, Song, Ying, Xie, Zhi-Hong, et al. Static and dynamic mechanical behavior of engineered cementitious composites with PP and PVA fibers[J].JOURNAL OF BUILDING ENGINEERING,2020,29.
- [15] Jin Hesong. Study on frost resistance (salt) and mechanical properties of polypropylene fiber reinforced cement-based composites[D].Southwest Jiaotong University, 2019 in chinese.
- [16] Zhu Deqi. Bending test and fractal characteristics of polypropylene fiber reinforced cementitious composites (PP-ECC)[D].Jilin University, 2020 in chinese.
- [17] Li V C, Mishra D K, Wu H C. Matrix design for pseudo strain-hardening fiber reinforced cementitious composites[J].Materials and Structures, 1995, 2(10): 586-595.
- [18] Zhang Lihui, Guo Liping, Sun Wei, Chen Zhengkai. Study on the deformation properties of ecological high ductility cement-based composites[J].Concrete, 2014 (8) : 82-87 in chinese.
- [19] General Administration of Quality Supervision. Concrete structure test method standard: GB/T 50152-2012[S].2012 in chinese.
- [20] Building materials. Test method for mechanical properties of high ductile fiber reinforced cement-based composites: JC/T 2461-2018[S].2018 in chinese.

- [21] Wang Xide, Ouyang Peng. Application of artificial neural network in the field of concrete structures [J].Low temperature building technology, 2022,44 (12): 75-78 in chinese.
- [22] Sinkhonde, David, Mashava, Destine, Bezabih, Tajebe, et al.Predicting the compressive strength of rubberized concrete incorporating brick powder based on MLP and RBF neural networks[J].Waste Management Bulletin,2025,3,(1):219-233.
- [23] Deng, Dayong,Wang, Jie,Deng, Zhixuan , et al.Rough set interpretation to RBF neural network[J].INTERNATIONAL JOURNAL OF MACHINE LEARNING AND CYBERNETICS,2025,1-20
- [24] Yuan, Zhongxia,Zheng, Wei,Qiao, Hongxia.Machine learning based optimization for mix design of manufactured sand concrete[J].CONSTRUCTION AND BUILDING MATERIALS,2025,467.